AIAA JOURNAL
Vol. 36, No. 2, February 1998

Design Approach for Minimizing Sound Power from Vibrating Shell Structures

E. W. Constans,* A. D. Belegundu,† and G. H. Koopmann‡
Pennsylvania State University, University Park, Pennsylvania 16802

A design approach for minimizing sound power radiation from vibrating thin shell structures is presented. The method couples finite element analysis for determining structural modes and vibrations with a boundary element/wave superposition code for determining sound power radiation. Noise reduction is accomplished herein by optimal placement and sizing of small point masses on the structure. These masses alter the critical mode shapes so as to reduce sound power. The simulated annealing technique is used to determine the location and/or magnitude of the point masses. A computer program has been developed for design. Design examples are presented with the use of the computer program.

I. Introduction

STRUCTURAL noise reduction is a field of great activity today. Until very recently, engineers were forced to design quiet structures through experimentation, a costly and time-consuming process. With the advent of inexpensive, powerful computers, however, the empirical method of designing quiet structures may soon be replaced by numerical modeling and optimization.

The work in this paper addresses the problem of reducing noise radiated from a vibrating shell structure. Some of the noisiest structures in airplanes and other forms of transportation involve thin plates or shells, usually as covering devices for mechanical components. For example, automobile engines employ sheet-metal valve covers, which protect the rocker-arm/valve assemblies from damage and seal in lubricating oil. Valve covers are usually made of relatively thin sheet metal and tend to radiate the engine noise outward from the engine rather than suppressing it. Other examples include fuselage skins and engine nacelles.

The design strategy presented is as follows. First, finite element analysis of the thin shell structure is performed. A modal superposition technique is used to obtain the forced response of the structure. Second, a boundary element/wave superposition method for determining sound power radiation is used; a computer code, POWER, which deals exclusively with exterior noise or radiated noise, has been recently developed.[1] Third, an optimizer based on the method of simulated annealing is used to optimally locate or size small point masses on the structure. These three steps, vibration analysis, radiated noise analysis, and optimization, are performed in an iterative loop. A design program, shell optimization for acoustic radiation (SOAR), has been developed to implement this strategy.

Two design examples are presented that were solved using the program. Physical interpretation has been given to the optimum designs obtained: The mode shapes have been altered so as to be weak radiators. This is described later in the paper.

This paper deals with reduction of exterior or radiated noise. Further, sound power is reduced through structural modifications rather than by use of active vibration control or acoustic sources (loudspeakers). Whereas active noise control has received much attention in the literature,[2–6] noise reduction through structural design is relatively new. Publications on noise reduction through structural optimization primarily have focused on interior noise in cabins and other enclosures[7–10] and on the exterior (radiated) noise from flat plates.[11–14] Very little work has been done on exterior noise from shells.[15] Some approaches address the acoustic problem by reducing the volume velocity on the surface of the vibrating body.[16] The contribution in this paper is to present a design approach for reducing sound power radiated from general shell structures. This work has been possible largely due to the development of the POWER code, which can compute radiated sound power from general three-dimensional shell structures.[1] The determination of acoustic radiation from flat plates, in contrast, is simpler as the Rayleigh integral may be used for sound power prediction.

Received Aug. 28, 1996; presented as Paper 96-4111 at the AIAA/USAF/NASA/ISSMO 6th Symposium on Multidisciplinary Analysis and Optimization, Bellevue, WA, Sept. 4–6, 1996; revision received Sept. 9, 1997; accepted for publication Sept. 22, 1997.

*Graduate Student, Department of Mechanical Engineering. Student Member AIAA.
†Associate Professor, Department of Mechanical Engineering. Senior Member AIAA.
‡Professor, Department of Mechanical Engineering.

II. Determination of Sound Power Level from Vibrating Shell Structures

Under consideration is a thin shell structure that is excited by harmonic nodal forces described by their magnitude and phase. The shell can have fixed, simply supported, or free boundary conditions. Point masses and springs may be attached to the shell, and proportional hysteritic damping is assumed. To model the acoustic power radiated by a shell structure requires two steps: vibration prediction and noise prediction. The vibration prediction section uses a finite element code to predict nodal velocities. These nodal velocities are entered into the noise prediction section, which uses a lumped parameter/wave superposition (LP/WS) method to predict sound power from the vibrating shell. Both portions of the program are described in greater detail next.

A. Finite Element Section

To predict sound power levels from a vibrating shell, it is first necessary to know the velocity $\boldsymbol{u}(x, y, z)$ at each point on the shell. The finite element code used here employs three-noded discrete Kirchhoff triangular shell elements (see Refs. 17 and 18 for details). If we wish to add nonstructural point masses to the global mass matrix (whose locations will be our design variables), we may use the equation

$$M_{n,n} = M_{n,n} + m_n \tag{1}$$

where m_n is the weight of the point mass. The element matrices are assembled to obtain global $\boldsymbol{K}$ and $\boldsymbol{M}$ matrices. To determine the vibration behavior of the shell, we must solve the differential equation $\boldsymbol{M}\ddot{\boldsymbol{x}} + (\boldsymbol{K} + i\boldsymbol{H})\boldsymbol{x} = \boldsymbol{F}e^{i\varpi t}$, where $\boldsymbol{x}$ is the nodal displacement vector, ϖ is the excitation frequency, $\boldsymbol{F}$ is the force vector, and $\boldsymbol{H} = \alpha\boldsymbol{K} + \beta\boldsymbol{M}$ is the damping matrix. Assuming a harmonic solution, and using modal superposition, the nodal velocities are

$$\dot{\boldsymbol{X}} = \sum_{j=1}^{m} i\varpi y_j \boldsymbol{Q}^j \tag{2}$$

where y_i is the modal participation factor and $\boldsymbol{Q}^j$ is the jth eigenvector. The resonance frequencies and mode shapes are determined by solving the eigenvalue problem $\boldsymbol{K}\boldsymbol{Q}^j = \omega_j^2 \boldsymbol{M}\boldsymbol{Q}^j$, which

is accomplished using the inverse iteration method.[19] The normal (w') components of $\dot{\boldsymbol{X}}$ are passed on to the sound power prediction portion of the program. From the normal velocities, volume velocities for each element are computed, leading to the determination of sound power as described next.

B. Boundary Element/Wave Superposition Method

Fahnline and Koopmann[1] describe a method of simulating the acoustic radiation of a structure by placing small acoustic point sources on the surface and matching the volume velocity boundary condition. Once the strengths of the small sources are known, the total sound power can be found by wave superposition. This enables a continuous structure to be simplified into a lumped parameter model, which can be analyzed using numerical methods. The LP/WS method replaces a vibrating structure with a collection of simple and dipole sources located on the surface of the structure. As with the finite element method, the structure is first discretized into surface elements, and the acoustic sources are placed at the centroids of the elements. To simplify matters, the nodal configuration used in the finite element section is used again in the LP/WS section; that is, the same mesh is used for vibration analysis and acoustic analysis. A brief description of the POWER code is given next.

To approximate the acoustic pressure field generated by this collection of simple and dipole sources, the acoustic fields from all of the sources are added together in the following manner:

$$\hat{p}(\boldsymbol{x}) \approx \sum_{m}^{N} \hat{s}_m P_m(\boldsymbol{x}) \tag{3}$$

where the caret notation indicates the complex amplitude of a function, $\hat{p}(\boldsymbol{x})$ is the acoustic pressure at the point $\boldsymbol{x}$, $P_m(\boldsymbol{x})$ is a basis function describing the pressure field of a single unit acoustic source, and $\hat{s}_m$ is the set of undetermined coefficients, which are used as source strengths for each of the sources. The idea is to determine those source strengths $\hat{s}_m$ that cause the volume velocities over each element to be equal to those obtained from the finite element code. The volume velocity over an element is defined as

$$\hat{u}_n = \iint_{S_n} \hat{v} \cdot \boldsymbol{n} \, \mathrm{d}S \tag{4}$$

where S_n is the surface area of an element, $\hat{\boldsymbol{v}}$ is the acoustic velocity, and $\boldsymbol{n}$ is the unit normal vector to the element. The volume velocity of an element may be thought of as the average normal velocity of the element multiplied by the surface area of the element. For this approximation to the boundary condition to be accurate, the normal velocity over the surface of the element must not vary by a great deal, so that it can be approximated as a piston vibrating with a velocity $\hat{v}_{\mathrm{av}}$. Thus, for this method to be accurate, the condition $ka < 1$ should be met, where k is the acoustic wave number (ω/c) and a is the largest characteristic dimension of the element. We use Euler's equation to rearrange Eq. (3) into the following form:

$$\hat{\boldsymbol{v}} \cdot \boldsymbol{n} \approx \frac{1}{ik\rho_a c} \sum_{m}^{N} \hat{s}_m \nabla P_m(\boldsymbol{x}) \cdot \boldsymbol{n} \tag{5}$$

where ρ_a is the average density of air and c is the speed of sound in air. Integrating over the surface of an element, we can write the elemental volume velocity in terms of the source strengths and basis functions

$$\hat{u}_n = \iint_{S_n} \hat{\boldsymbol{v}} \cdot \boldsymbol{n} \, \mathrm{d}S \approx \frac{1}{ik\rho_a c} \sum_{m}^{N} \hat{s}_m \iint_{S_n} \nabla P_m(\boldsymbol{x}) \cdot \boldsymbol{n} \, \mathrm{d}S \tag{6}$$

In this manner, the acoustic coupling between elements is taken into account. To avoid nonuniqueness problems (discussed in much greater detail in the paper by Fahnline and Koopmann[1]), we choose as our basis functions the following:

$$P_m(\boldsymbol{x}) = \alpha \hat{g}(\boldsymbol{x}, \boldsymbol{q}_m) + \beta \nabla \hat{g}(\boldsymbol{x}, \boldsymbol{q}_m) \cdot \boldsymbol{n} \tag{7}$$

where the $\hat{g}$ is the free-space Green's function, $\boldsymbol{q}_m$ is the location of the acoustic source, $\boldsymbol{x}$ is a field point, and $\boldsymbol{n}$ is the vector normal to the acoustic source (that is, normal to the element). The first term in Eq. (7) represents the acoustic pressure field of a unit simple source, whereas the second term represents the acoustic field of a dipole source. The coupling constants α and β determine the relative strengths of the simple and dipole sources.

Substituting our basis function into the expression for volume velocity [Eq. (6)],

$$\hat{u}_n = \frac{1}{ik\rho_a c} \sum_{m=1}^{N} \hat{s}_m \iint_{S_n} \nabla \{ \alpha_m \hat{g}(\boldsymbol{x}, \boldsymbol{q}_m) + \beta_m \nabla \hat{g}(\boldsymbol{x}, \boldsymbol{q}_m) \cdot \boldsymbol{n}_{q_m} \} \cdot n \, \mathrm{d}S \tag{8}$$

We may also write this in matrix form as

$$\boldsymbol{u} = \boldsymbol{U}\boldsymbol{s} \tag{9}$$

where $\boldsymbol{s}$ is the vector of source strengths. All of the terms in the expression for the $\boldsymbol{U}$ matrix are known and may be calculated using numerical integration techniques. When the source and field points are far apart, standard Gaussian quadrature may be used. For points located very near each other, a more complicated semianalytical scheme similar to the one described by Duong[20] is applied. The volume velocity vector $\boldsymbol{u}$ is calculated from the nodal velocities given by the finite element solution. Without going into the details, the power output of a collection of simple and dipole sources is given by

$$\Pi_{\mathrm{av}} = \tfrac{1}{2} \boldsymbol{s}^H \boldsymbol{S} \boldsymbol{s} \tag{10}$$

where the superscript H denotes the Hermitian transpose and the matrix $\boldsymbol{S}$ is a Hermitian matrix that relates the acoustic power to the source strengths.

To summarize, the LP/WS section first reads in the nodal velocities calculated by the finite element section of the program. These nodal velocities are then averaged over each element and multiplied by the elemental areas to produce volume velocities. The volume velocities provide the needed boundary condition for predicting sound power with LP/WS. The final output from the LP/WS section is the total radiated sound power. Note that structural–acoustic coupling is neglected in this analysis.

III. Optimization Technique

When choosing an optimization algorithm, one must decide whether a gradient or nongradient routine should be used. Gradient methods have the advantage of (typically) converging on an optimal solution quite rapidly, especially if the objective function is well behaved. Belegundu et al.,[12] Hambric,[21] and Keane[22] have discussed that, for vibration and acoustic response optimization, nongradient optimization methods are attractive compared to gradient methods. This is because of the presence of local minima, which arise owing to the changes in resonance conditions (mode switching) with changes in design variables. Here, a simulated annealing algorithm is used for optimization. The method of simulated annealing is especially suitable for problems with multiple local minima owing to its ability to find a global minimum.[23,24]

Simulated annealing is called a stochastic optimization method because it moves in random directions when searching for an optimum. It begins its search at a user-specified design point and then moves in a random direction, searching for a minimum. If the move was in the downhill direction, i.e., if the sound power at the new design is lower than in the original design, the new design is accepted and the algorithm moves again in another random direction. If the move was uphill, however, the new design point has a certain probability of being accepted anyway, depending on the size of the uphill move and a parameter called the temperature. This is called the metropolis criterion. In this fashion, the algorithm may escape local minima to converge onto a global minimum.

To understand why the algorithm is called simulated annealing, consider the annealing process. When a metal is at a high temperature, the atoms within the metal are relatively free to move about in random directions. As the temperature decreases, the atoms become more and more constrained to move within a smaller region, until freezing occurs. Thus, metals find the optimal atomic packing by first moving in random directions at high temperatures and then having the range of movement decrease as the temperature decreases. The simulated annealing algorithm works in much the same way, with very large, random steps being taken in the beginning and

smaller steps (with less likelihood of uphill steps being accepted) being taken as the algorithm proceeds.

As design variables in the computer program, we may choose location/weight of discrete point masses, shell thicknesses, and composite properties, to name a few. In this work, we have chosen point masses as these are simple to build and test in a laboratory to validate the computer simulations.

IV. Design Examples

Two design examples are presented. The first problem involves the vibration of a flat plate. This problem has been discussed in the literature and is presented for validation of the methodology presented and of the SOAR code. The second design example deals with a vibrating shell and is directly related to the main contribution of this paper, viz., a methodology for minimizing sound power radiated from shells. Also, these two problems presented in detail can serve as benchmarks for further study.

A. Clamped Plate Problem

The flat plate problem to be described has been optimized in an earlier publication by Wodtke and Koopmann.[25] This example has been chosen simply to validate the SOAR program. The approach used by Wodtke and Koopmann[25] is entirely different from the SOAR program used here; they determine sound power based on the Rayleigh–Ritz approach. Also, they have corroborated the optimum results obtained from the Rayleigh–Ritz technique experimentally.

The objective for this problem is to minimize the sound power at the fifth resonance of a clamped plate driven at its center with a shaker. Figure 1 shows a schematic diagram of the plate, which is made of aluminum ($E = 71.7$ GPa, $\nu = 0.31$, $\rho = 2790$ kg/m^3) with dimensions $290 \times 290 \times 1.016$ mm^3. The plate is driven with a harmonic force $F = 0.018$ N uniformly at all frequencies. According to the finite element analysis the first five modes occur at 131.6, 214.5, 214.5, 314.5, and 342.9 Hz, respectively. Of these, the first and fifth modes are noise producing, whereas the others are quiet due to volume velocity cancellations. Again, the objective is the reduction of noise from the fifth mode only. The design variable is the magnitude of four equally sized lumped masses placed at the quarter-points of the plate (Fig. 2).

To model this arrangement using the SOAR program, a finite element mesh was created using 13 nodes on each side of the plate for a total of 169 nodes. The shaker was modeled as a discrete external stiffness. For greater accuracy, we have modeled the additional bulk stiffness created by the air enclosed in the box as follows.

The pressure increase caused by the deflection of the shell is

$$\delta p \approx \frac{\kappa P_0 \delta V}{V_0} \tag{11}$$

where

$$\delta V = \iint_S w'(x', y')\, \mathrm{d}S \tag{12}$$

is the volume change inside the box, $w'(x', y')$ is the normal displacement at any point on the shell, κ is the ratio of specific heats for air, and P_0 and V_0 are the ambient pressure and initial box volume, respectively. The work done by compressing the air is

$$U = \int_{\hat{v}} \frac{\kappa \delta V P_0}{V_0}\, \mathrm{d}\delta V = \frac{\kappa P_0}{2V_0}(\delta V)^2 \tag{13}$$

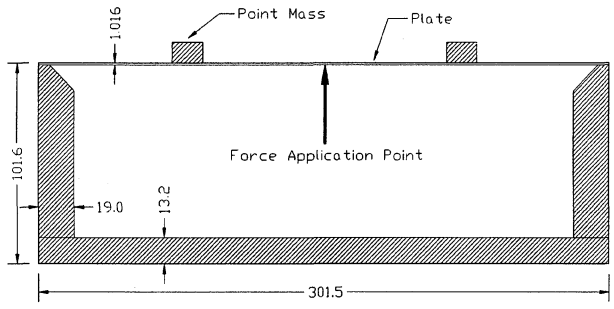

Fig. 1 Schematic diagram of plate problem; all dimensions are in millimeters.

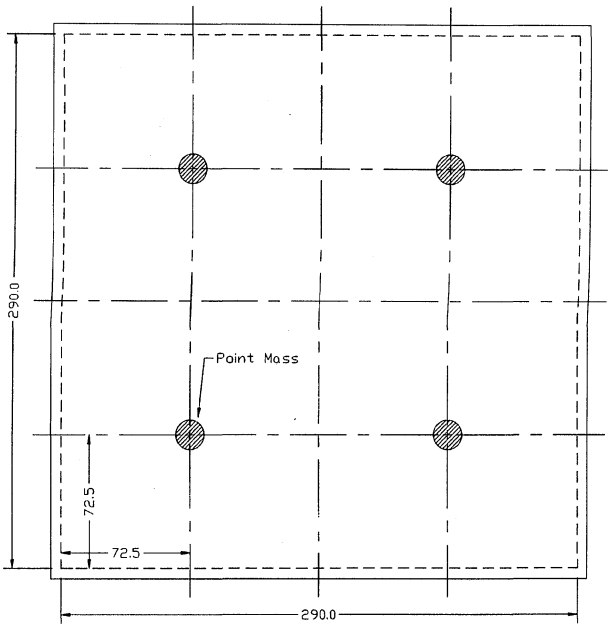

Fig. 2 Locations of point masses on flat plate.

Using finite element shape functions for $w'(x', y')$, the stiffness matrix can be determined from Eq. (13).

We note that the natural frequencies of standing waves inside the box are

$$\omega_{lmn} = c\sqrt{(l\pi/L_x)^2 + (m\pi/L_y)^2 + (n\pi/L_z)^2} \tag{14}$$

where L_x, L_y, and L_z are the interior dimensions of the box. The longest interior dimension of the box in question is 263.5 mm. With speed of sound equal to 343 m/s, the first natural frequency inside the box is approximately 650 Hz. Because the fifth mode of the plate covering the box lies in the range of 200–350 Hz, depending on the value of the masses added to the plate, standing modes of the air inside the box will not play a role in this design study.

Optimization results are now discussed. The optimal mass at the four quarter-point locations found using SOAR is 31.2 g. The sound power at the fifth resonance before optimization for the flat plate was 78.01 dB at 342.9 Hz. This was reduced to 45.00 dB at 212.8 Hz after optimization. Thus, the total reduction at the fifth mode was 33 dB. Note that the resonance frequency of the fifth mode will change with increasing mass; peak tracking was used to follow this mode during optimization. Figure 3 shows the sound power spectrum plot without and with the optimal masses. The peak associated with mode 5 has disappeared. Also, see Fig. 4 for how the sound power varies with mass magnitude.

To understand why the power has reduced with this optimal mass, it is informative to examine the mode shapes of the fifth mode before and after optimization. Figure 5 shows these mode shapes. As can be seen, the size of the center peak has been changed so as to provide total volume velocity cancellation with the four smaller corner peaks. The optimal mass magnitude found by SOAR is within 12.8% of the value of 35.8 g in Ref. 25 obtained using the Rayleigh–Ritz method. The results from SOAR are in general agreement with those obtained in Ref. 25 and with the experimental results in that paper.

B. Semicylindrical Shell Problem

A semicylindrical shell is shown in Fig. 6. The shell is open at the ends, is clamped along the two lower edges, and is driven harmonically with magnitude $F = 0.8$ N at its top center in the vertical direction. The shell is made of aluminum with $E = 71.7$ GPa, $\nu = 0.31$, and $\rho = 2790$ kg/m^3. The thickness of the shell is 2 mm.

Instead of determining the optimal magnitudes for the point masses as before, the program was instructed to find the optimum locations of two 35.8-g masses that minimize sound power radiated at the first five modes. That is, the objective function is defined as

$$\min\{W = W_1 + W_2 + W_3 + W_4 + W_5\} \tag{15}$$

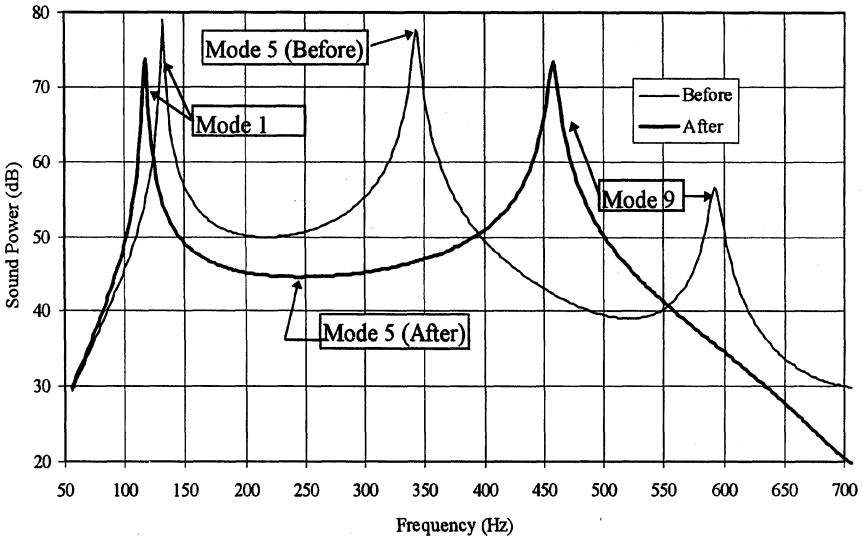

Fig. 3 Sound power of plate before and after optimization (ref. 10^{-12} W).

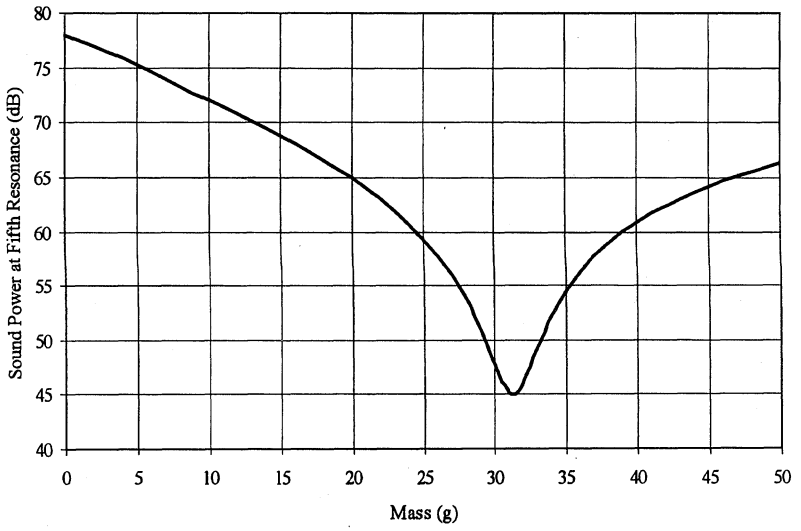

Fig. 4 Optimization curve for plate problem.

where W_i is the sound power at the ith resonant frequency. Equation (15) represents the objective of minimizing power over a broadband of excitation frequencies because, when damping is low, most of the power is radiated at structural resonances. The locations of the masses were constrained to lie on the finite element nodes; the locations of the two masses are the design variables in the simulated annealing optimizer. Each of the masses represents less than 10% of the total shell weight; therefore, correct mass placement is critical.

Mode Shapes and Sound Power Levels Before Optimization

The first three mode shapes of the shell are shown in Fig. 7. The first mode shape is a horizontal swaying mode and produces very little sound power, because the driving force is in the vertical direction. The second mode (piston type) produces the largest amount of sound power. The third mode (rocking or seesaw type) creates only a small amount of noise, due to the effect of volume velocity cancellation. That is, one side of the shell moves up and compresses the air while the other side moves downward and rarefies the same amount of air. The overall effect is that very little net volume velocity is created. The fourth and fifth modes (not shown) are not strong noise producers, again due to volume velocity cancellation.

Optimum Mass Locations and Physical Explanation

Figure 8 shows the optimal locations for the point masses found by the sound power minimization program. It is noteworthy that the

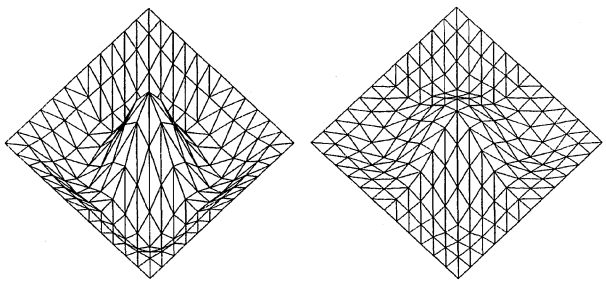

Fig. 5 Shapes of fifth mode before and after optimization.

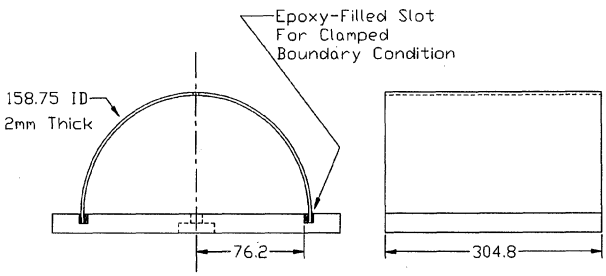

Fig. 6 Half-cylindrical shell; all dimensions are in millimeters.

Table 1 Sound power of half-cylinder before and after optimization

	Before optimization		After optimization	
Mode	Frequency, Hz	Power, dB	Frequency, Hz	Power, dB
1	325.1	29.5	299.8	26.8
2	676.4	84.7	541.9	72.9
3	740.7	69.1	580.6	71.3
4	1184.3	62.5	1139.9	57.2
5	1345.5	61.7	1345.5	56.8
Total		84.8		75.3

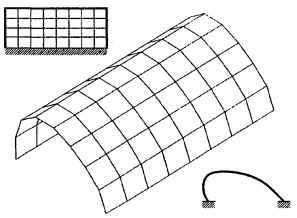

Mode 1: sway

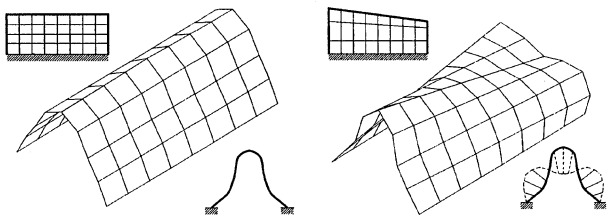

Mode 2: piston **Mode 3: rocking**

Fig. 7 First three mode shapes of half-cylinder before optimization.

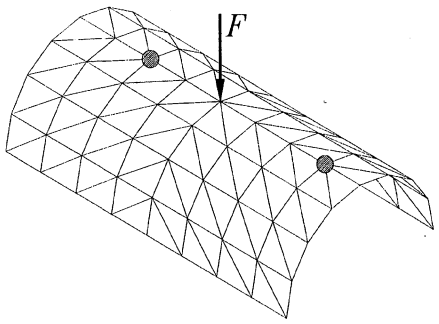

Fig. 8 Optimal mass locations for shell.

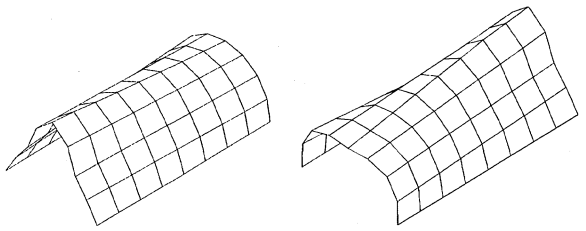

Fig. 9 Second and third mode shapes after optimization, both rocking.

optimal mass placement is asymmetric with respect to the transverse axis of the cylinder even though the problem is symmetric. To understand this phenomenon, observe Fig. 9, which shows the second and third mode shapes of the half-cylinder with the optimal mass configuration. As can be seen, the piston and rocking modes have both been converted into asymmetric rocking type modes, both of which produce only a small amount of sound power. Table 1 shows the sound power levels and natural frequencies of each mode before and after optimization. As can be seen, a total reduction of 9.6 dB is predicted by the SOAR code. Experimental confirmation of these results is currently in progress.

V. Conclusion

The development of the POWER code for predicting radiated sound power from general three-dimensional structures has motivated this work. The POWER code has been integrated with a finite element code and a simulated annealing optimizer to result in the SOAR program. This program has been applied to two examples: 1) sound power reduction from a flat plate with magnitudes of masses as design variables and 2) sound power reduction from a semicylindrical shell with locations of point masses as variables. In both cases, the design program has yielded designs that were effective in quieting vibration modes. Importantly, the optimum results have been shown to have a clear physical explanation, viz., that mode shapes have been altered in such a way that volume velocity cancellations have taken place resulting in quieter modes of vibration. Thus, the optimization approach here achieves modal tailoring as opposed to simply detuning or shifting the natural frequencies outside a certain band.

A sound power minimization methodology for arbitrarily shaped shell structures has been demonstrated. The method presented can enable the designer to reduce sound power levels from shell structures, such as automobile valve covers and gear box casings, or can enable the designer to design a casing that is placed over a sound source, such as a compressor. This work represents an extension of previous work in exterior noise carried out for flat plates. Future possibilities lie in more general material tailoring, viz., use of plate thicknesses, composites, and ribs or other stiffeners.

Acknowledgment

The authors thank John Fahnline of the Applied Research Laboratory at Pennsylvania State University for his valuable assistance in the use of the POWER code.

References

[1]Fahnline, J. B., and Koopmann, G. H., "Lumped Parameter Model for the Acoustic Power Output from a Vibrating Structure," *Journal of the Acoustical Society of America*, Vol. 100, No. 6, 1996, pp. 3539–3547.

[2]Nelson, P. A., and Elliott, S. J., "The Minimum Power Output of a Pair of Free Field Monopole Sources," *Journal of Sound and Vibration*, Vol. 105, 1986, pp. 173–178.

[3]Nelson, P. A., Curtis, A. R. D., Elliott, S. J., and Bullmore, A. J., "The Minimum Power Output of Free Field Point Sources and the Active Control of Sound," *Journal of Sound and Vibration*, Vol. 116, 1987, pp. 397–414.

[4]Elliott, S. J., Joseph, P., Nelson, P. A., and Johnson, M. E., "Power Output Minimization and Power Absorption in the Active Control of Sound," *Journal of the Acoustical Society of America*, Vol. 90, No. 5, 1991, pp. 2501–2512.

[5]Cunefare, K. A., and Koopmann, G. H., "Global Optimum Active Noise Control: Surface and Far-Field Effects," *Journal of the Acoustical Society of America*, Vol. 90, No. 1, 1991, pp. 365–373.

[6]Cunefare, K. A., and Koopmann, G. H., "A Boundary Element Approach to Optimization of Active Noise Control Sources on Three Dimensional Structures," *Journal of Vibration and Acoustics*, Vol. 113, 1991, pp. 387–394.

[7]Bernhard, R. J., "A Finite Element Method for Synthesis of Acoustical Shapes," *Journal of Sound and Vibration*, Vol. 98, No. 1, 1985, pp. 55–65.

[8]Pal, C., and Hagiwara, I., "Dynamic Analysis of a Coupled Structural–Acoustic Problem: Simultaneous Multimodal Reduction of Vehicle Interior Noise Level by Combined Optimization," *Finite Elements in Analysis and Design*, Vol. 14, 1993, pp. 225–234.

[9]Engelstad, S. P., Cunefare, K. A., Crane, S., and Powell, E. A., "Optimization Strategies for Minimum Interior Noise and Weight Using FEM/BEM," *Proceedings of Inter-Noise '95*, 1995.

[10]Browell, J., Glaves, A., and Stark, R., "Keeping Noise in Bounds," *Mechanical Engineering*, Jan. 1995, pp. 84–86.

[11]Lamancusa, J. S., "Numerical Optimization Techniques for Structural–Acoustic Design of Rectangular Panels," *Computers and Structures*, Vol. 48, No. 4, 1993, pp. 661–675.

[12]Belegundu, A. D., Salagame, R. R., and Koopmann, G. H., "A General Optimization Strategy for Sound Power Minimization," *Structural Optimization*, Vol. 8, 1994, pp. 113–119.

[13]St. Pierre, R. L., Jr., and Koopmann, G. H., "A Design Method for Minimizing the Sound Power Radiated from Plates by Adding Optimally Sized, Discrete Masses," *Journal of Mechanical Design*, Vol. 117, 1995, pp. 243–251.

[14]Naghshineh, K., Koopmann, G. H., and Belegundu, A. D., "Material Tailoring of Structures to Achieve a Minimum Radiation Condition," *Journal of the Acoustical Society of America*, Vol. 92, No. 2, 1992, pp. 841–855.

[15]Hambric, S. A., "Structural–Acoustic Optimization of a Point-Excited Submerged Cylindrical Shell," *Proceedings of the 4th AIAA/USAF/NASA/OAI Symposium on Multidisciplinary Analysis and Optimization*, AIAA, Washington, DC, 1992, pp. 1096–1103.

[16]Milsted, M. G., Zhang, T., and Hall, R. A., "A Numerical Method for Noise Optimization of Engine Structures," *Proceedings of the Institution of Mechanical Engineers*, Vol. 207, 1993, pp. 135–143.

[17]Cook, R. D., Malkus, D. S., and Plesha, M. E., *Concepts and Applications of Finite Element Analysis*, 3rd ed., Wiley, New York, 1989.

[18]Zienkiewicz, O. C., *The Finite Element Method*, 3rd ed., McGraw–Hill, New York, 1983, p. 329.

[19]Chandrupatla, T. R., and Belegundu, A. D., *Introduction to Finite Elements in Engineering*, Prentice–Hall, Englewood Cliffs, NJ, 1991, p. 343.

[20]Duong, T. H., "A Finite Element Method for the Double-Layer Potential Solutions of the Neumann Exterior Problem," *Mathematical Methods in Applied Science*, Vol. 2, 1980, pp. 191–208.

[21]Hambric, S. A., "Sensitivity Calculations for Broad-Band Acoustic Radiated Noise Design Optimization Problems," *Journal of Vibration and Acoustics*, Vol. 118, 1996, pp. 529–532.

[22]Keane, A. J., "Experiences with Optimizers in Structural Design," *Adaptive Computing in Engineering Design and Control*, Plymouth, England, UK, 1994, pp. 14–27.

[23]Szykman, S., and Cagan, J., "Synthesis of Optimal Non-Orthogonal Routes," *ASME Design Engineering Technical Conferences*, Vol. 1, American Society of Mechanical Engineers, New York, 1995, pp. 431–438.

[24]Corana, A., et al., "Minimizing Multimodal Functions of Continuous Variables with the 'Simulated Annealing' Algorithm," *ACM Transactions on Mathematical Software*, Vol. 13, No. 3, 1987, pp. 262–280.

[25]Wodtke, H. W., and Koopmann, G. H., "Quieting Plate Modes with Optimally Sized Point Masses—A Volume Velocity Approach," DE Vol. 84, No. 3, American Society of Mechanical Engineers, New York, 1995, pp. 647–654.

S. Glegg
Associate Editor